The Journal of Neuroscience, May 15, 2000, *20*(10):3785–3797

Distribution, Targeting, and Internalization of the sst_4 Somatostatin Receptor in Rat Brain

Matthias Schreff,[1] Stefan Schulz,[1] Manuela Händel,[1] Gerburg Keilhoff,[2] Holger Braun,[1] Gabriela Pereira,[1] Marcus Klutzny,[1] Harald Schmidt,[1] Gerald Wolf,[2] and Volker Höllt[1]

Departments of [1]Pharmacology and Toxicology and [2]Medical Neurobiology, Otto-von-Guericke University, 39120 Magdeburg, Germany

Somatostatin mediates its diverse physiological effects through a family of five G-protein-coupled receptors (sst_1–sst_5); however, knowledge about the distribution of individual somatostatin receptor proteins in mammalian brain is incomplete. In the present study, we have examined the regional and subcellular distribution of the somatostatin receptor sst_4 in the rat CNS by raising anti-peptide antisera to the C-terminal tail of sst_4. The specificity of affinity-purified antibodies was demonstrated using immunofluorescent staining of HEK 293 cells stably transfected with an epitope-tagged sst_4 receptor. In Western blotting, the antiserum reacted specifically with a broad band in rat brain, which migrated at ~70 kDa before and ~50 kDa after enzymatic deglycosylation. sst_4-Like immunoreactivity was most prominent in many forebrain regions, including the cerebral cortex, hippocampus, striatum, amygdala, and hypothalamus. Analysis at the electron microscopic level revealed that sst_4-expressing neurons target this receptor preferentially to their somatodendritic domain. Like the sst_{2A} receptor, sst_4-immunoreactive dendrites were often closely apposed by somatostatin-14-containing fibers and terminals. However, unlike the sst_{2A} receptor, sst_4 was not internalized in response to intracerebroventricular administration of somatostatin-14. After percussion trauma of the cortex, neuronal sst_4 receptors progressively declined at the sites of damage. This decline coincided with an induction of sst_4 expression in cells with a glial-like morphology. Together, this study provides the first description of the distribution of immunoreactive sst_4 receptor proteins in rat brain. We show that sst_4 is strictly somatodendritic and most likely functions in a postsynaptic manner. In addition, the sst_4 receptor may have a previously unappreciated function during the neuronal degeneration–regeneration process.

Key words: somatostatin; somatostatin receptor subtypes; antibodies; immunocytochemistry; internalization; trauma

The neuropeptide somatostatin exerts a variety of effects in the CNS and peripheral nervous system. Two biological active forms have been identified in mammals, the cyclic tetradecapeptide somatostatin-14 (SS-14) and the N terminally extended somatostatin-28 (SS-28), both of which are derived from a common precursor molecule (Brazeau et al., 1973). Recently, a somatostatin-like peptide, cortistatin, with a high degree of homology but a more restricted distribution, has been isolated (de Lecea et al., 1996, 1997). In the CNS, somatostatin acts as neurotransmitter and neuromodulator to regulate neuronal firing in a predominantly inhibitory manner and plays a role in the modulation of complex behaviors, such as motor activity and cognition (for review, see Gillies, 1997).

The physiological effects of somatostatin are mediated through a family of seven transmembrane-spanning G-protein-coupled receptors (for review, see Bell and Reisine, 1993; Hoyer et al., 1995). Five genes encoding distinct somatostatin receptor subtypes, termed sst_1–sst_5, have so far been cloned in humans and other species (Bruno et al., 1992; Kluxen et al., 1992; Meyerhof et al., 1992; O'Carroll et al., 1992; Vanetti et al., 1992, 1993; Yamada et al., 1992; Yasuda et al., 1992; Rohrer et al., 1993). Several different radioligands have been used to investigate the overall distribution of somatostatin binding sites in mammalian brain; however, none of the somatostatin receptor ligands used in these studies was sufficiently selective to allow definitive discrimination between the various receptor subtypes (Uhl et al., 1985; Martin et al., 1991; Holloway et al., 1996). Elucidation of the cellular and subcellular localization of the various somatostatin receptor subtypes would provide important insights into somatostatinergic transmission in the CNS. So far, only the somatostatin receptor subtypes sst_1, sst_{2A}, sst_{2B}, and sst_3 have been localized by immunocytochemistry in mouse and rat brain (Dournaud et al., 1996, 1998; Schindler et al., 1997, 1999; Helboe et al., 1998, 1999; Händel et al., 1999; Schulz et al., 1998b,c).

The somatostatin receptor sst_4 binds SS-14 and SS-28 with high affinity and exhibits virtually no affinity for the synthetic somatostatin analogs seglitide and octreotide (Rohrer et al., 1993). When stably expressed in Chinese hamster ovary or human embryonic kidney 293 (HEK 293) cells, sst_4 mediates inhibition of forskolin-stimulated cAMP formation and a prolonged activation of mitogen-activated protein kinase (Rohrer et al., 1993, Bito et al., 1994, Sellers, 1999). In the CNS, sst_4 mRNA is highly expressed in the cerebral cortex, hippocampus, amygdala, and hypothalamus (Bito et al., 1994; Harrington et al., 1995; Perez and Hoyer, 1995). In the present study, we raised antisera against a

Received Dec. 13, 1999; revised Feb. 22, 2000; accepted Feb. 25, 2000.

This work was supported by Deutsche Forschungsgemeinschaft Grants SCHU 924/4-1 (S.S.) and SFB 426 TPA2 (V.H.), European Commission Grant QRTL-1999-00908 (S.S.), Volkswagen-Stiftung Grant I/75 172 (S.S.), Kultusministerium des Landes Sachsen/Anhalt Grant 1908A/0025 (S.S.), and a grant from the Bundesministerium für Bildung und Forschung Schwerpunkt Neurotraumatologie (V.H.). We thank Dana Wiborny, Dora Nüβ, Evelyn Kahl, and Karina Schäfer for excellent technical assistance and Dr. H.-J. Kreienkamp for kindly providing sst_3T7tag and sst_4T7tag expression vectors.

Correspondence should be addressed to Volker Höllt, Department of Pharmacology and Toxicology, Otto-von-Guericke University, Leipziger Strasse 44, 39120 Magdeburg, Germany. E-mail: volker.hoellt@medizin.uni-magdeburg.de.

synthetic peptide corresponding to the C-terminal tail of sst_4 and used these antibodies to explore the distribution, targeting, and internalization of the sst_4 receptor protein in the brain of adult rats.

MATERIALS AND METHODS

Generation of anti-peptide antisera. Rabbit polyclonal antisera were generated against the C-terminal portion of sst4. The identity of the 23 amino acid sequence was CQQEPVQAEPGCKQVPFTKTTTF, which corresponds to residues 362–384 of the mouse sst_4 receptor. The peptide was custom synthesized by Gramsch Laboratories (Schwabhausen, Germany), purified by HPLC, and coupled via an N terminally added cysteine and an SMCC (succinimidyl 4-[*N*-maleimidomethyl] cyclohexane-1-carboxylate) linker to keyhole limpet hemocyanin. The conjugate (500 μg/ml) was emulsified with an equal volume of Freund's complete adjuvant for the first and Freund's incomplete adjuvant for subsequent immunizations. Two rabbits (6001 and 6002) were injected at 4 week intervals, and serum was obtained 2 weeks after immunizations beginning with the second injection.

Dot-blot analysis and immunoaffinity purification. The specificity of the antisera, as well as possible cross-reactivity with other somatostatin receptor subtypes, was initially tested in dot-blot assays. Serial dilutions of the unconjugated peptides corresponding to the C-terminal sequences of sst_1, sst_{2A}, sst_{2B}, sst_3, sst_4, and sst_5 were blotted onto nitrocellulose membranes. The identity of the peptides was as follows: ESGGVFRNGTCASRISTL, which corresponds to residues 374–391 of the mouse and rat sst_1; ETQRTLLNGDLQTSI, which corresponds to residues 355–369 of the human, mouse, and rat sst_{2A}; ADNSKTGEEDTMAWV, which corresponds to residues 329–343 of the rat sst_{2B}; TAGDKASTLSHL, which corresponds to residues 417–428 of the mouse and rat sst_3; CQQEPVQAEPGCKQVPFTKTTTF, which corresponds to residues 362–384 of the mouse sst_4; and QATLPTRSCEANGLMQTSRI, which corresponds to residues 344–363 of the rat sst_5 receptor. Membranes were then incubated with the sst_4 antisera 6001 and 6002 at dilutions ranging from 1:1000 to 1:20,000 for 60 min at room temperature (RT). Blots were developed using peroxidase-conjugated secondary antibodies (1:5000) and enhanced chemiluminescence (Amersham Pharmacia Biotech, Braunschweig, Germany).

Immunoaffinity columns were constructed by cross-linking of the sst_4 C-terminal peptide CQQEPVQAEPGCKQVPFTKTTTF to iodoacetyl agarose columns, and purification of anti-sst_4 antiserum (6002) was performed using the SulfoLink Kit (Pierce, Rockford, IL) as recommended by the manufacturer. Eluted fractions of purified IgG were pooled and rescreened using dot-blot analysis. In all subsequent experiments, affinity-purified anti-sst_4 antibodies were used.

Western blot analysis and deglycosylation experiments. HEK 293 cells were stably transfected with rat sst_1, rat sst_{2A}, T7-tagged rat sst_3, T7-tagged rat sst_4, or rat sst_5 receptors using the calcium phosphate precipitation method (Koch et al., 1998). The T7 epitope tag was added at the N-terminal tail of sst_3 and sst_4 with a sequence encoding 11 amino acids of the T7 major capsid protein (MASMTGGQQMG) using PCR (expression vectors for T7-tagged sst_3 and T7-tagged sst_4 were kindly provided by Dr. H.-J. Kreienkamp, (Institut für Zellbiochemie und klinische Neurobiologie, Universität Hamburg, Hamburg, Germany) (Roth et al., 1997). Approximately 1.5×10^6 cells were transfected with 20 μg of plasmid DNA. Cells were selected in the presence of 500 μg/ml G418 (Life Technologies, Eggenstein, Germany). Membranes were prepared from stably transfected HEK 293 cells, as well as from several rat brain regions, including olfactory bulb, cortex, striatum, hippocampus, and cerebellum. Tissue was lysed in homogenization buffer (5 mM EDTA, 3 mM EGTA, 250 mM sucrose, and 10 mM Tris-HCl, pH 7.6, containing 1 mM phenylmethylsulfonylfluoride, 1 μM pepstatin, 10 μg/ml leupeptin, and 2 μg/ml aprotinin). The homogenate was spun at $500 \times g$ for 5 min at 4°C to remove unbroken cells and nuclei. Membranes were then pelleted at $20,000 \times g$ for 30 min at 4°C and resuspended in lysis buffer (150 mM NaCl, 5 mM EDTA, 3 mM EGTA, and 20 mM HEPES, pH 7.4, containing 4 mg/ml dodecyl-β-maltoside and proteinase inhibitors as above). The lysate was centrifuged at $20,000 \times g$ for 30 min at 4°C, and when indicated, glycoproteins were partially purified using wheat germ lectin agarose (WGA) (Vector Laboratories, Burlingame, CA). The supernatant was incubated with 100 μl of WGA beads for 90 min at 4°C. Beads were washed five times, and adsorbed glycoproteins were eluted with SDS sample buffer (62.5 mM Tris-HCl, pH 6.8, 2% SDS, 20% glycerol, 200 mM DL-dithiotreitol, and 0.005% bromphenol blue) for 20 min at 60°C. Deglycosylation experiments were performed using peptide *N*-glycosidase F (PNGase F) according to the manufacturer's protocol (New England Biolabs, Beverly, MA). Either crude membrane proteins (100 μg/lane) or WGA extracts purified from 500 μg membrane proteins were subjected to 8% SDS-PAGE and immunoblotted onto nitrocellulose. Blots were incubated with affinity-purified anti-sst_4 (1 μg/ml) or mouse monoclonal anti-T7 tag antibody (1:5000; Novagen, Madison, WI) overnight at 4°C and then developed using peroxidase-conjugated secondary antibodies and enhanced chemiluminescence. For adsorption controls, anti-sst_4 antibody was preincubated with 10 μg/ml of its cognate peptide for 2 hr at RT.

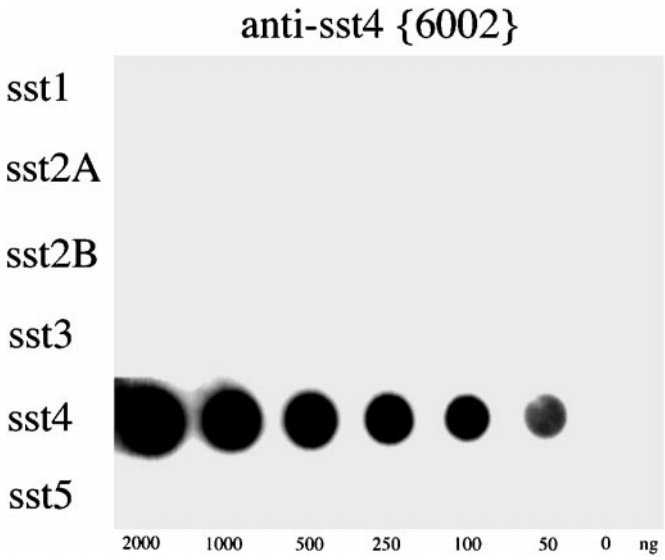

Figure 1. Immunodot-blot analysis of the specificity of the anti-sst_4 antiserum. Serial dilutions (0–2000 ng) of the peptides corresponding to the C-terminal regions of sst_1, sst_{2A}, sst_{2B}, sst_3, sst_4, and sst_5 were blotted onto a nitrocellulose membrane and incubated with affinity-purified anti-sst_4 antibody (6002) at a concentration of 1 μg/ml. The blot was subsequently incubated with peroxidase-conjugated secondary antibodies and developed using enhanced chemiluminescence.

Immunocytochemistry. Wild-type HEK 293 cells or HEK 293 cells stably transfected with T7-tagged sst_3 or T7-tagged sst_4 receptors were grown on coverslips overnight. Primary dissociated cultures of rat hippocampus and cortex were prepared from embryonic day 19 fetuses and grown on coverslips for 1–2 weeks as described previously (Papa et al., 1995). For internalization studies, cells were treated with 100 nM SS-14 for 10, 30, 45, or 60 min and fixed with 4% paraformaldehyde and 0.2% picric acid in 0.1 M phosphate buffer, pH 7.4, for 1 hr at RT. Coverslips were washed several times in TPBS (10 mM Tris-HCl, 10 mM phosphate buffer, 137 mM NaCl, and 0.05% thimerosal, pH 7.4) and preincubated with TPBS containing 0.3% Triton X-100 and 3% normal goat serum (NGS) for 1 hr at RT. Primary neuronal cultures were then incubated with either affinity-purified anti-sst_4 (1 μg/ml) or anti-sst_{2A} (1 μg/ml). HEK 293 cells were incubated with a mixture of affinity-purified anti-sst_4 (1 μg/ml) and mouse monoclonal anti-T7 antibodies (1:5000) in TPBS containing 0.3% Triton X-100 and 1% NGS overnight at 4°C. For adsorption controls, primary antibodies were preincubated with homologous peptides (10 μg/ml) for 2 hr at RT. For single immunofluorescence, bound primary antibodies were detected with biotinylated anti-rabbit IgG antibodies (Vector Laboratories), followed by cyanine 3.18 (Cy3)-conjugated streptavidin (Amersham Pharmacia Biotech). For double immunofluorescence labeling, bound primary antibodies were detected with biotinylated anti-rabbit IgG antibodies, followed by a mixture of cyanine 2.18 (Cy2)-conjugated streptavidin and cyanine 5.18 (Cy5)-conjugated anti-mouse antibodies (Jackson ImmunoResearch, West Grove, PA). Cells were then dehydrated in graded alcohols, cleared in xylol, and permanently mounted in DPX (Fluka, Neu-Ulm, Germany).

For light microscopy, male Wistar rats ($n = 8$, 200–230 gm; Tierzucht Schönwalde, Germany) were deeply anesthetized with chloral hydrate and transcardially perfused with Tyrode's solution, followed by Zamboni's fixative containing 4% paraformaldehyde and 0.2% picric acid in 0.1 M phosphate buffer, pH 7.4. In a separate set of experiments, rats received an intracerebroventricular injection of 1 μg of SS-14 either 30

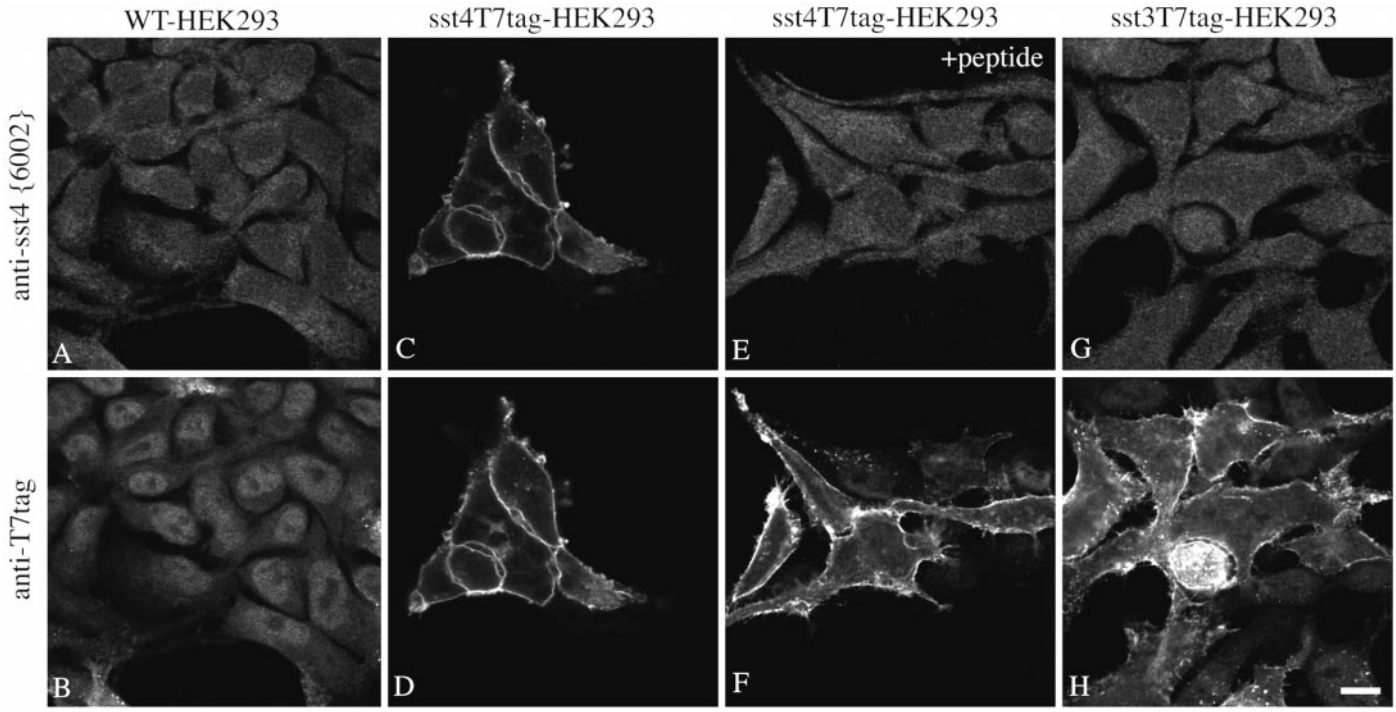

Figure 2. Characterization of the anti-sst_4 antiserum using stably transfected HEK 293 cells. Double immunofluorescent labeling and confocal imaging of wild-type HEK 293 cells (*A*, *B*) and HEK 293 cells transfected with a construct coding for sst_4T7tag (*C–F*) or sst_3T7tag (*G*, *H*) using a mixture of the anti-sst_4 antiserum (6002) and the mouse monoclonal anti-T7 antibody. For absorption controls, this mixture was preincubated with 10 μg/ml of the homologous sst_4 peptide (*E*, *F*). Note that the anti-sst_4 antiserum yielded prominent immunofluorescence localized at the level of the plasma membrane only in sst_4T7tag-expressing HEK 293 cells but not in wild-type or sst_3T7tag-expressing HEK 293 cells. This staining is completely abolished by preincubation with homologous peptide. *WT*, Wild-type. Scale bar, 15 μm.

($n = 3$) or 60 ($n = 3$) min before vascular perfusion. Control animals received an equal volume of vehicle injection ($n = 6$). Brains and spinal cords were rapidly dissected and post-fixed in the same fixative for 2 hr at RT. For all animal procedures, ethical approval was sought before the experiments according to the requirements of the *German National Act on the Use of Experimental Animals*. Tissue was cryoprotected by immersion in 30% sucrose for 48 hr at 4°C before sectioning using a freezing microtome. Free-floating sections (30–40 μm) were washed in TPBS, placed in 50% ethanol for 30 min to block endogenous peroxidase activity, and incubated in 3% NGS in TPBS with 0.3% Triton X-100 for 1 hr. Tissue sections were then incubated with affinity-purified anti-sst_4 (1 μg/ml in TPBS containing 0.3% Triton X-100 and 1% NGS) for 48–72 hr at RT. Staining of primary antibody was detected using the biotin amplification procedure as described previously (Schulz et al., 1998b). Briefly, tissue sections were transferred to biotinylated goat anti-rabbit IgG (1:1000 in TPBS containing 0.3% Triton X-100 and 1% NGS; Vector Laboratories) for 2 hr and incubated with avidin-biotinylated peroxidase complex (ABC) solution for 1 hr. Bound peroxidase was reacted with biotinylated-tyramine solution for 20 min, which was then visualized with streptavidin-Cy3 for single immunofluorescence.

For double labeling of the sst_4 receptor with somatostatin, glial, or neuronal marker proteins, the anti-sst_4 antibody (2.5 μg/ml) was coincubated for 48–72 hr at RT with the following mouse monoclonal antibodies: anti-somatostatin (clone K121, 1:50; Biomeda, Foster City, CA), anti-microtubule-associated protein 2 (MAP-2) (1:2000; Sternberger Monoclonals, Baltimore, MD), anti-neurofilament (1:2000; SMI-312; Sternberger Monoclonals), or anti-glial fibrillary acidic protein (GFAP) (1:2000; Boehringer Mannheim, Mannheim, Germany). Binding of primary antibodies was detected with biotinylated anti-rabbit IgG antibodies (Vector Laboratories), followed by a mixture of Cy2-conjugated streptavidin (Amersham Pharmacia Biotech) and Cy5-conjugated anti-mouse IgG antibodies (Jackson ImmunoResearch).

Double labeling of the sst_4 receptor with other somatostatin receptor subtypes required staining of the sections with two different primary antibodies raised in the same host species. Thus, tissue sections were first incubated with very low concentrations of anti-sst_{2A} (6291; 1:20,000), anti-sst_{2B} (5574; 1:40,000), or anti-sst_3 (7986; 1:30,000) antibodies, all of which have been raised and extensively characterized in our laboratory (Schulz et al., 1998a,b,c; Händel et al., 1999). Staining of these antibodies was then detected using the biotin amplification procedure as described above. Sections were washed and incubated with affinity-purified anti-sst_4 antibody at a concentration of 2.5 μg/ml overnight, followed by a final incubation with a mixture of Cy2-conjugated streptavidin (Amersham Pharmacia Biotech) and Cy5-conjugated anti-rabbit IgG antibodies (Jackson ImmunoResearch). Sections were mounted onto chrome alum gelatin-subbed glass slides and dehydrated in graded alcohols, cleared in xylol, and coverslipped with DPX. For immunocytochemical controls, the primary antibody was omitted, replaced by preimmune sera, or adsorbed with several concentrations ranging from 1 to 10 μg/ml homologous or heterologous peptides for 2 hr at RT. Specimens were examined using a Leica (Heidelberg, Germany) TCS-NT laser scanning confocal microscope equipped with a krypton–argon laser. Cy2 was imaged with 488 nm excitation and 500–560 bandpass emission filter, Cy3 with 568 nm excitation and 570–630 nm bandpass emission filters, and Cy5 with 647 nm excitation and 665 nm long-pass emission filters.

For electron microscopy, male Wistar rats (200–230 gm) were anesthetized as above and perfusion-fixed (4% paraformaldehyde, 0.2% picric acid, and 0.2% glutaraldehyde in 0.1 M phosphate buffer, pH 7.4). The brains were post-fixed in 4% paraformaldehyde for 2 hr at RT. Blocks of brain tissue were washed for 2 hr in 0.1 M phosphate buffer, immersed in 10% sucrose for 1 hr, and then placed in 20% sucrose overnight at 4°C. Subsequently, tissue was snap frozen in liquid nitrogen and thawed in 0.1 M phosphate buffer. Seventy micrometer vibratome sections were collected, washed in TPBS, and transferred into 50% ethanol for 30 min. After 1 hr blocking in TPBS containing 3% NGS, tissue sections were incubated with anti-sst_4 antibody (1–2.5 μg/ml in TPBS containing 1% NGS) for 72 hr. Sections were subsequently transferred to biotinylated anti-rabbit IgG antibodies and ABC solution. All incubations were performed at RT and without Triton X-100. Immunolabeling was visualized with DAB-glucose oxidase for 10–30 min. Sections were post-fixed with 1% osmium tetroxide, *en bloc* contrasted with 1% uranyl acetate, dehydrated in a series of graded alcohols, and flat-embedded in Durcupan. Ultrathin sections (40–50 nm) were cut with a diamond knife using an ultracut MT 7000 (RMC, Tuscon, AZ). Sections

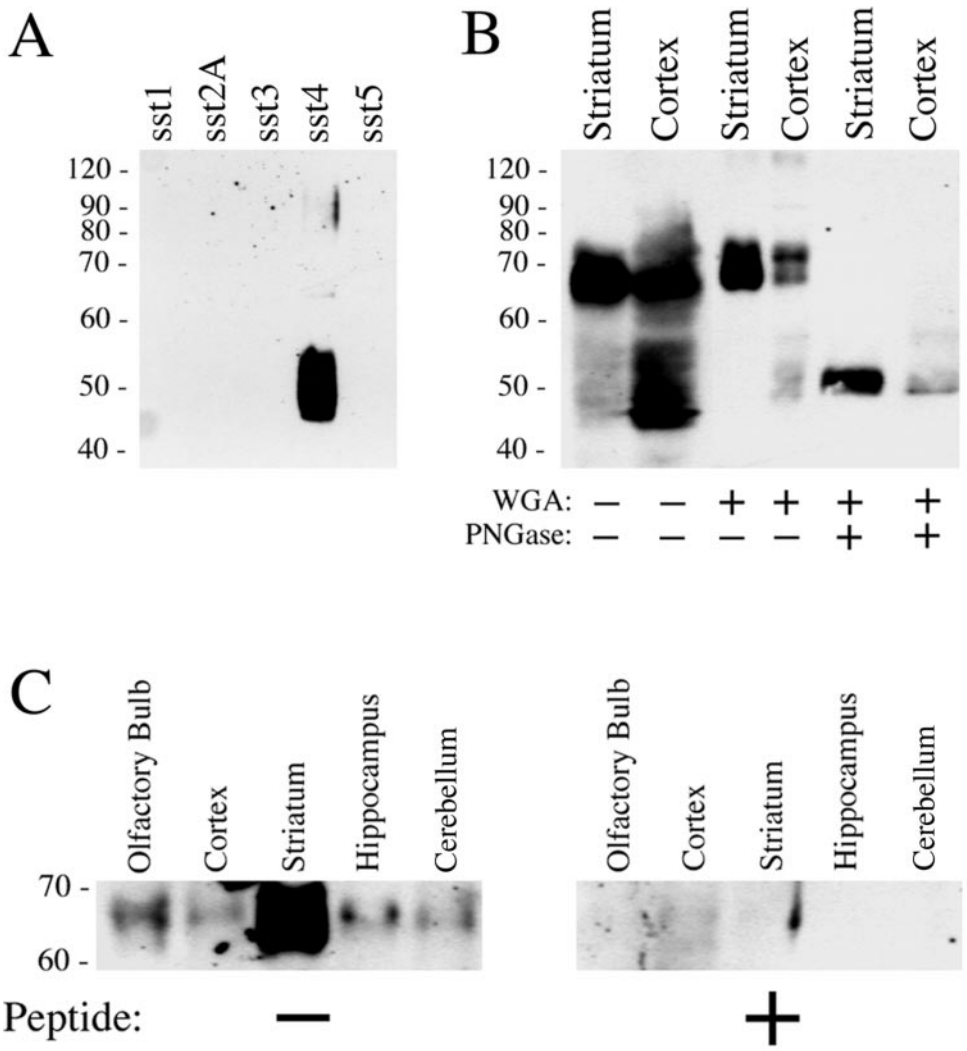

Figure 3. Western blot analysis of sst_4-immunoreactivity in transfected HEK 293 cells and rat brain. *A*, Membrane preparations from HEK 293 cells transfected with sst_1, sst_{2A}, sst_3, sst_4, or sst_5 were separated on an 8% SDS polyacrylamide gel and blotted onto nitrocellulose. Membranes were then incubated with affinity-purified anti-sst_4 antibodies (6002) at a concentration of 1 μg/ml. *B*, Crude membrane preparations, WGA-purified preparations, or PNGase F-treated WGA extracts prepared from striatum and cortex were separated on an 8% SDS polyacrylamide gel and blotted onto nitrocellulose. Membranes were then incubated with affinity-purified anti-sst_4 antibodies (6002) at a concentration of 1 μg/ml. *C*, WGA extracts prepared from the olfactory bulb, cortex, striatum, hippocampus, and cerebellum were separated on an 8% SDS polyacrylamide gel and blotted onto nitrocellulose. Membranes were then incubated with affinity-purified anti-sst_4 antibodies (6002) at a concentration of 1 μg/ml in either the absence (*left panel*) or presence (*right panel*) of the peptide antigen (10 μg/ml). Blots were developed using enhanced chemiluminescence. Ordinate, Migration of protein molecular weight markers ($M_r \times 10^{-3}$).

were collected onto copper mesh grids and examined with a Zeiss (Oberkochen, Germany) 900 electron microscope.

Cortical percussion trauma. Unilateral contusion was made to the cortex essentially as described by Bernert and Turski (1996). Briefly, the contusion device for the rat brain injury consisted of a 40 cm long-stainless steel tube. The device was kept perpendicular to the surface of the scull and guided a falling weight onto the foot plate resting on the surface of the dura. A force of 380 gm/cm^2 produced by a 20 gm weight was selected to produce brain contusion. Adult male Wistar rats were anesthetized with tribromoethanol (260 mg/kg, i.p.; Aldrich, Deisenhofen, Germany). A craniotomy was performed, and the center of the foot plate was stereotaxically positioned 1.5 mm posterior and 2.5 mm lateral to the bregma. Unilateral contusion was made to the cortex. Animals were killed by vascular perfusion after 8 ($n = 6$) or 24 ($n = 6$) hr as described above. Sham controls ($n = 6$) had identical anesthesia and surgery without impact.

RESULTS

Characterization of antisera

Antisera were raised in rabbits against a synthetic peptide corresponding to residues 362–384 of the C terminus of sst_4. Specificity of the antisera was initially monitored using immunodot-blot analysis. After four boost injections, both rabbit antisera (6001 and 6002) developed a titer against their immunizing peptide. When several dilutions of these antisera were tested, the anti-sst_4 antiserum 6002 detected quantities as low as 50 ng of its cognate peptide but not the peptides corresponding to other somatostatin receptor subtypes at a dilution of 1:20,000. Thus, the sst_4 antiserum 6002 was subjected to immunoaffinity purification, and the resulting IgG preparation was rescreened using immunodot-blot analysis (Fig. 1).

The antiserum (6002) was further characterized using immunofluorescent staining of stably transfected HEK 293 cells. When wild-type HEK 293 cells or either sst_4T7tag- or sst_3T7tag-transfected cells were stained with a mixture of the anti-sst_4 antibody (6002) and the mouse monoclonal anti-T7 tag antibody and processed for double immunofluorescence, the anti-sst_4 antiserum yielded prominent immunofluorescence localized at the level of the plasma membrane only in HEK 293 cells bearing the sst_4 receptor (Fig. 2*A*,*C*,*G*). This staining pattern was completely blocked by preincubation of the antiserum with homologous peptide (Fig. 2*E*). In contrast, the anti-T7 antibody yielded prominent immunofluorescence localized at the level of the plasma membrane in HEK 293 cells transfected with either sst_4T7tag or sst_3T7tag but not in wild-type cells (Fig. 2*B*,*D*,*H*). This staining was not affected by preincubation with the sst_4 homologous peptide (Fig. 2*F*). In addition, the anti-sst_4 antiserum 6002 did not stain HEK 293 cells stably expressing the sst_1, sst_{2A}, sst_3, or sst_5 receptors (data not shown).

The specificity of the antibody was then tested by Western blotting analysis. When membrane preparations from stably

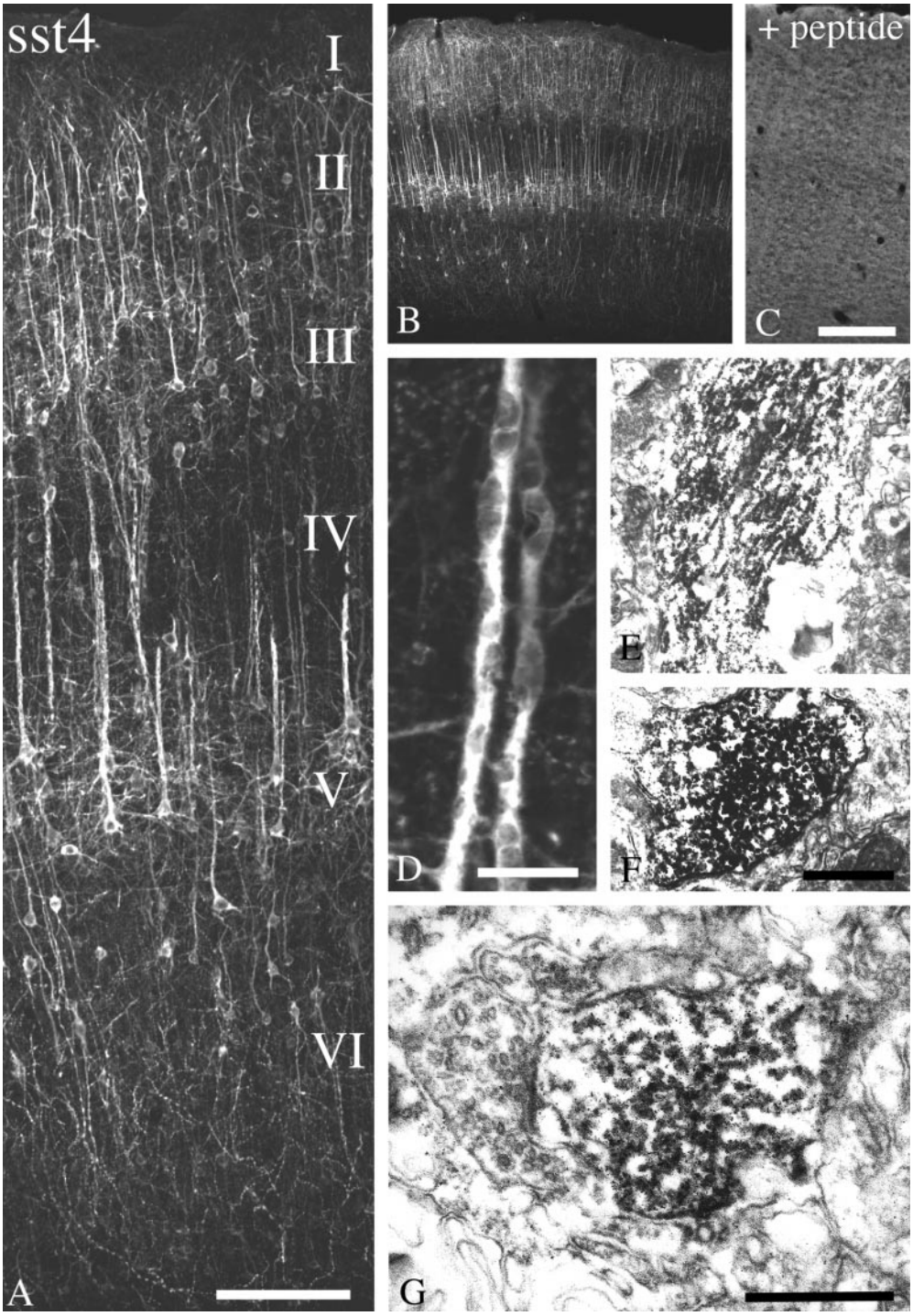

Figure 4. Immunofluorescent and electron micrographs showing the regional and subcellular localization of sst_4-Li in rat neocortex. *A*, *B*, *D*, Coronal rat brain section immunofluorescently stained with affinity-purified anti-sst_4 antibodies (6002). *C*, Corresponding adsorption control. The anti-sst_4 antibody was preincubated with 10 μg/ml of its cognate peptide. *E*, *F*, Rat brain sections from cortical layer IV were processed for immunoperoxidase detection of the anti-sst_4 antibody. *G*, Rat brain sections from cortical layer I were processed for immunoperoxidase detection of the anti-sst_4 antibody. Note that sst_4-Li is enriched throughout the layers of the cerebral cortex with prominent labeling of pyramidal cells in layers II/II and V, as well as their primary dendrites. This staining pattern is completely neutralized by preincubation with the immunizing peptide. At the electron microscopic level, immunoperoxidase product was mostly intracellular in large apical pyramidal cell dendrites in layer IV. In layer I in which sst_4-immunopositve dendrites project into and ramify, immunolabeling was more densely distributed along neuronal plasma membranes. The neuronal profiles containing sst_4-Li were dendrites and symmetrical synapses. Scale bars: *A*, 50 μm; *B*, *C*, 200 μm; *D*, 10 μm; *E*, *F*, 1.5 μm; *G*, 0.4 μm.

transfected HEK 293 cells were analyzed, and the anti-sst_4 antibody 6002 detected a broad band migrating at 45–55 kDa only in membrane extracts from sst_4T7tag-expressing cells but not in extracts from HEK 293 cells expressing other somatostatin receptor subtypes (Fig. 3*A*). The anti-T7 tag antibody detected a single band of identical molecular weight in sst_4T7tag-transfected cells (data not shown). In contrast, Western blot analysis of striatal and cortical membranes revealed a major band migrating at 65–72 kDa and a smaller band with migration properties similar to that seen in sst_4-expressing HEK 293 cells (Fig. 3*B*). After partial purification of *N*-glycosylated proteins from rat brain membranes using WGA, only the 65–72 kDa band was detected (Fig. 3*B*). When these WGA extracts were subjected to enzymatic deglycosylation using PNGase F, a sharp band of ~48–50 kDa was detected (Fig. 3*B*). These data are consistent with the majority of rat brain sst_4 receptors being heavily glycosylated with the sst_4 receptors heterologously expressed in HEK 293 cells being either nonglycosylated or only partially glycosylated. In addition, WGA extracts from selected brain regions were subjected to Western blot analysis (Fig. 3*C*, *left panel*), showing that immunoreactive (IR) sst_4 receptors are present in high levels in the striatum, olfactory bulb, and cerebral cortex and to a lesser

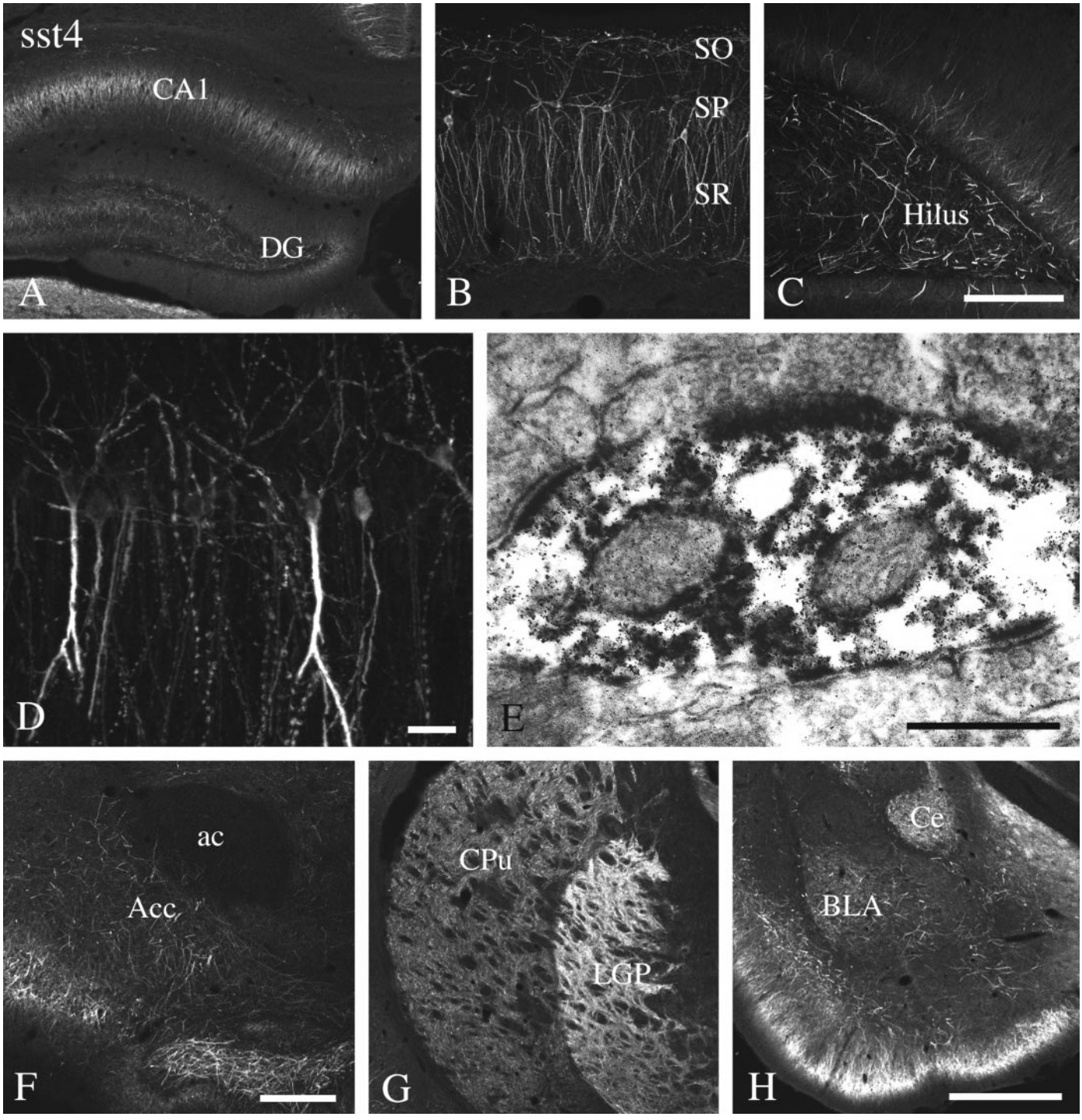

Figure 5. Immunofluorescent and electron micrographs showing the regional and subcellular localization of sst_4-Li in rat forebrain. *A–D*, *F–H*, Coronal rat brain section immunofluorescently stained with affinity-purified anti-sst_4 antibodies (6002). *E*, Rat brain sections from the hippocampal CA1 region were processed for immunoperoxidase detection of the anti-sst_4 antibody. Note that sst_4-Li is enriched in the hippocampal formation with high levels found in the Ammon's horn and the hilar region of the dentate gyrus. sst_4-Li was also distributed along neuronal processes in the nucleus accumbens, striatum, and amygdala. At the electron microscopic level, immunoperoxidase product was always postsynaptic, and some instances of immunolabeling at asymmetrical synapses were found in the hippocampal CA1 region (*E*). *ac*, Anterior commissure; *Acc*, nucleus accumbens, *BLA*, basolateral amygdaloid nucleus; *Ce*, central amygdaloid nucleus, *CPu*, caudate-putamen; *DG*, dentate gyrus; *LGP*, lateral globus pallidus; *SO*, stratum oriens; *SP*, stratum pyramidale, *SR*, stratum radiatum. Scale bars: *A*, *G*, *H*, 250 μm; *B*, *C*, 50 μm; *D*, 10 μm; *E*, 0.2 μm; *F*, 100 μm.

extent in the hippocampus and cerebellum. These bands were no longer detected when the antiserum was preincubated with its cognate peptide (Fig. 3*B*, *right panel*).

When brain sections of adult rats were immunocytochemically stained, the sst_4 antibody revealed a selective staining pattern with high levels of sst_4-like immunoreactivity (Li) in many forebrain regions, including the olfactory bulb, cerebral cortex, hippocampus, striatum, and amygdala (Figs. 4, 5). This immunostain-

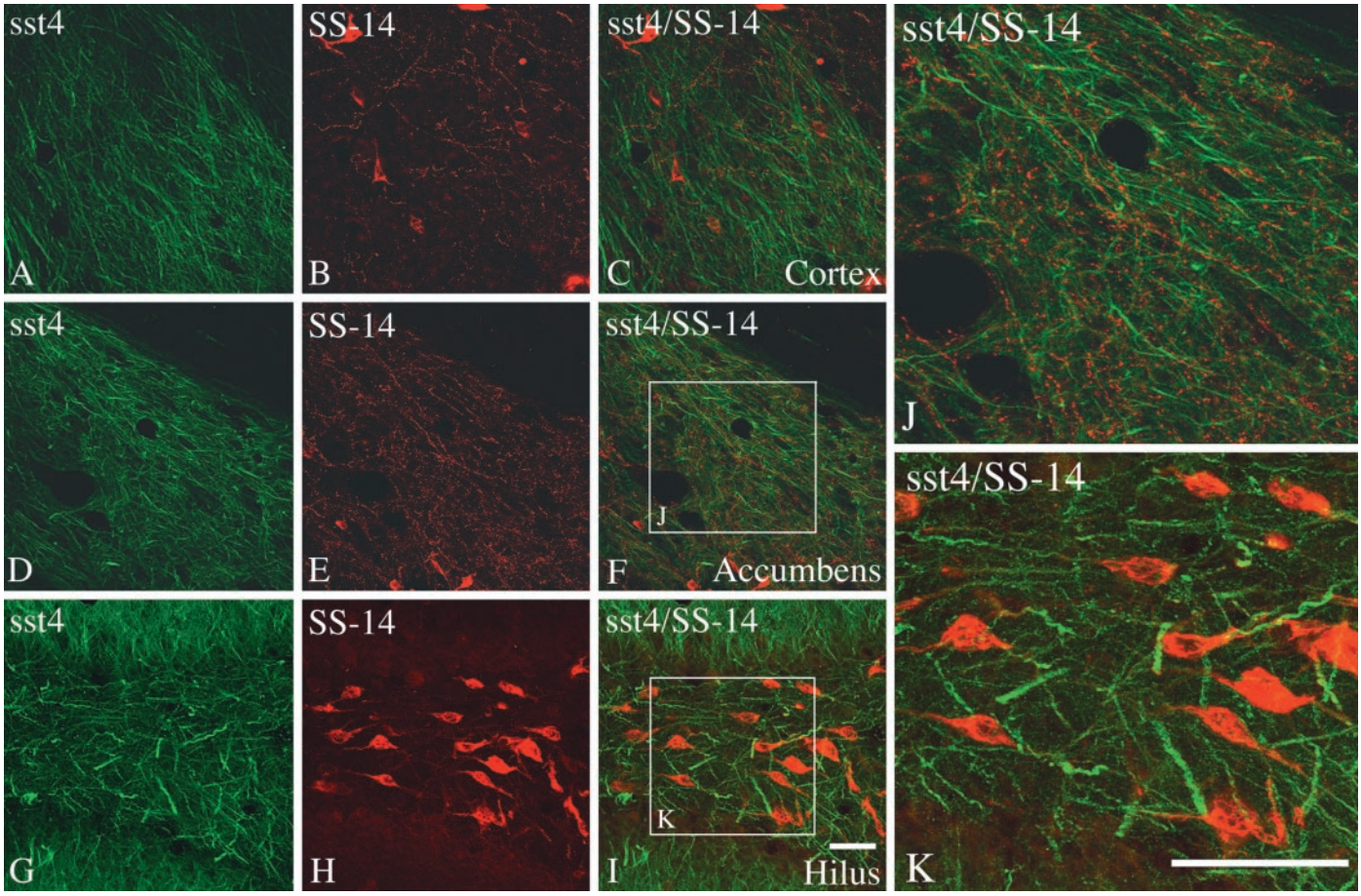

Figure 6. Immunofluorescent confocal images of rat brain sections showing the spatial relationship of the sst_4 receptor and SS-14. *A–K,* Coronal rat brain sections double stained for sst_4-Li (*green*) and SS-14-LI (*red*). Note that, in the cerebral cortex and nucleus accumbens, sst_4-immunoreactive dendrites were often closely apposed by SS-14-containing fibers and terminals (*C*, *F*, *J*). In contrast, in the hilar region of the dentate gyrus, immunoreactive sst_4 receptors appeared to decorate distal processes of SS-14-positive interneurons (*I*, *K*). Scale bars: *A–I*, 50 μm; *J*, *K*, 25 μm.

ing was completely abolished by preabsorption of the sst_4 antibody with homologous, but not with heterologous, peptides (10 μg/ml) (Fig. 4*B*,*C*).

Somatostatin receptor 4-Li is prominent in rat forebrain

sst_4-Li was abundant throughout the rat forebrain (Figs. 4, 5). In the main olfactory bulb, sst_4-Li was most dense in the external plexiform layer but was also seen in the glomerular, mitral cell, and internal granular layers. sst_4-Li was also present in other structures of the olfactory system, including the anterior olfactory nucleus, olfactory tubercle, and islands of calleja. Prominent sst_4-Li was found throughout the layers (I–VI) of the neocortex in which it decorated neuronal somata and processes, including those of pyramidal cells in layers III and V (Fig. 4*A*). Although the majority of these large layer V pyramidal cells are presumably glutamatergic, sst_4-Li was seen on parvalbumin-containing (presumably GABAergic) neurons in layer IV. In the hippocampal formation, sst_4-Li was detected in the Ammon's horn with similar densities throughout CA1–CA3 and in the hilar region of the dentate gyrus (Fig. 5*A–C*). In the Ammon's horn, sst_4-Li was present on apical dendrites of pyramidal cells in the stratum radiatum and scattered interneurons. In general, staining of the primary dendrites of both cortical and hippocampal pyramidal cells appeared to be more dense then the staining of the somata of these neurons (Figs. 4*D*, 5*D*). sst_4-Li was also seen on scattered fibers within the hilar region of dentate gyrus (Fig. 5*C*). sst_4-Li was distributed along neuronal processes in the striatum, nucleus accumbens, and globus pallidus, with the highest density in the globus pallidus (Fig. 5*F*,*G*). In the amygdala, sst_4-immunoreactive fibers and somata were abundant in the cortical, central, and basolateral nuclei (Fig. 5*H*). In addition, sst_4-Li was moderately dense in distinct nuclei of the thalamus. Moderate to strong fiber labeling was seen in the habenula, as well as in the lateral hypothalamic area. sst_4-Li was present on Purkinje cells within the cerebellar cortex. Scattered sst_4-IR fibers were seen in the ventral areas of the medulla and spinal cord. In general, sst_4-Li was most prominent in the forebrain, and the density of sst_4-Li progressively decreased within the caudal brain regions.

To further elucidate the subcellular targeting of the sst_4-immunoreactive elements, double-labeling experiments of sst_4 with neuronal and glial markers were performed. In virtually all brain regions examined, sst_4-Li was colocalized with MAP-2 but not with neurofilament or GFAP, indicating that the sst_4 receptor protein is predominantly targeted to the somatodendritic domain of neurons (data not shown). To elucidate the subcellular sites for sst_4 functions more precisely, we used the immunoperoxidase method and electron microscopy. When large apical dendrites from cortical pyramidal cells of layer V were examined, much of

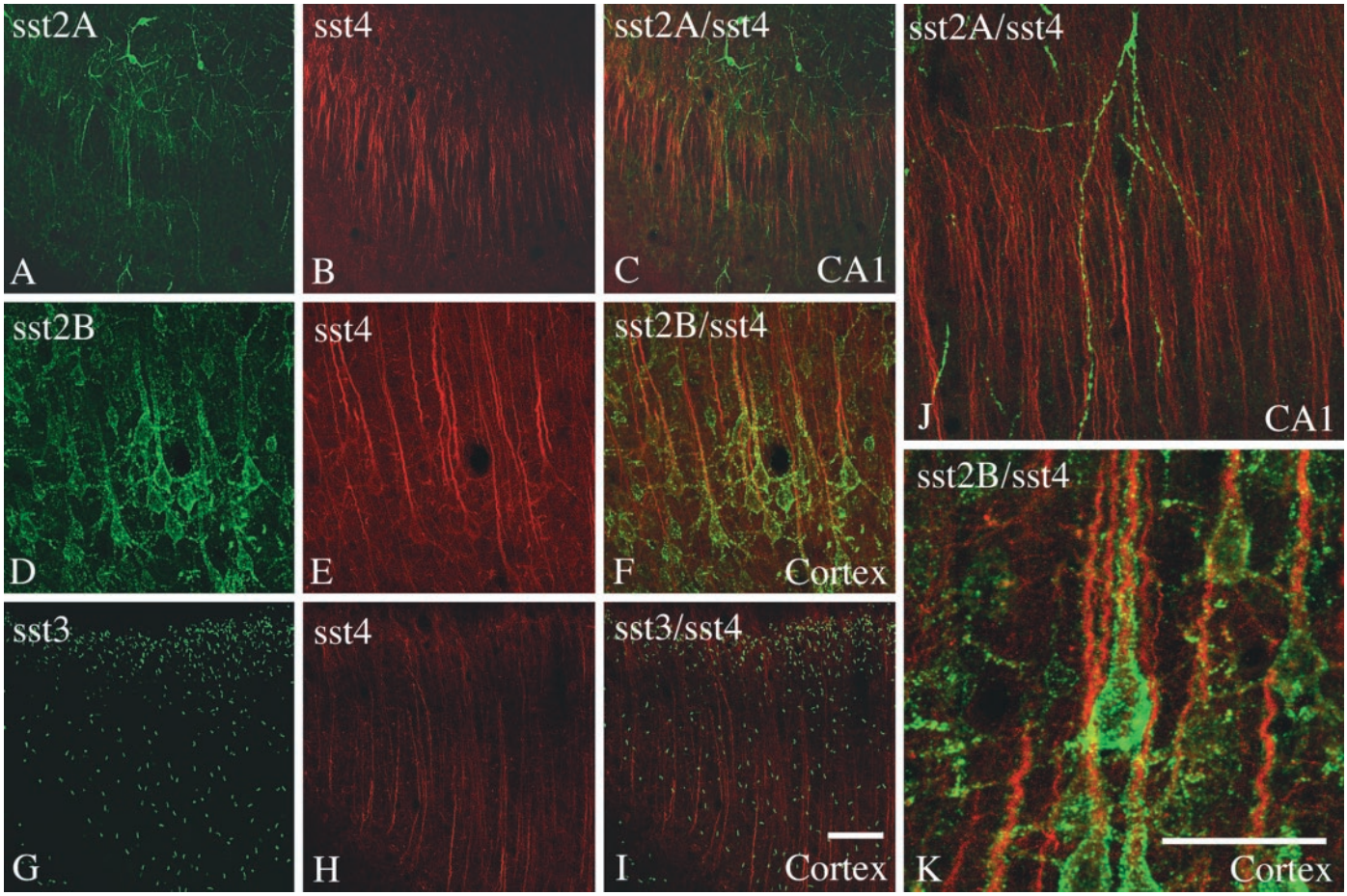

Figure 7. Immunofluorescent confocal images of rat brain sections showing the spatial relationships between the sst_4 receptor and other somatostatin receptor subtypes. *A–C*, *J*, Coronal rat brain sections double stained for sst_{2A}-Li (*green*) and sst_4-Li (*red*). *D–F*, *K*, Coronal rat brain sections double stained for sst_{2B}-Li (*green*) and sst_4-Li (*red*). *G–I*, Coronal rat brain sections double stained for sst_3-Li (*green*) and sst_4-Li (*red*). Note that a high degree of colocalization was seen between sst_4-Li and sst_{2B}-Li in layer V cortical pyramidal cells (*K*). Whereas sst_{2B}-Li was distributed in a patch-like manner along the soma and proximal dendrites, sst_4-Li was most dense at the distal portion of the apical dendrites of these neurons (*K*). No such colocalization was observed between either sst_4 and sst_{2A} or sst_4 and sst_3. Scale bars: *A–I*, 50 μm; *J*, *K*, 25 μm.

the immunolabeling appeared to be intracellular and not confined to the neuronal plasma membrane (Fig. 4*D–F*). We also examined cortical layer I in which sst_4-immunopositve pyramidal cells of layers III and VI project into and ramify. In contrast to that seen in the deeper layer of the cortex, sst_4-positve immunolabeling was frequently more densely distributed along neuronal plasma membranes. The neuronal profiles containing sst_4-Li were dendrites and symmetrical synapses (Fig. 4*G*). This suggests that the predominant intracellular localization of the immunoperoxidase reaction product in large pyramidal cell dendrites may originate from sst_4 receptors being transported to or from their targets. In addition, very similar results were obtained for the striatum and hippocampus in which sst_4-Li was exclusively postsynaptic. However, it should be noted that, in the hippocampal formation, some instances of sst_4-positive immunolabeling of asymmetrical presumably excitatory synapses were found (Fig. 5*E*).

Spatial relationship of somatostatin receptor 4 to its ligand somatostatin

To explore the relationship between the sst_4 receptor and its ligand(s), we used double immunofluorescence using the affinity-purified rabbit anti-sst_4 antibody (6002) and the mouse monoclonal anti-SS-14 antibody (clone K121). Immunodot-blot analysis revealed that the K121 antibody, which was generated to SS-14, does not discriminate between somatostatin and cortistatin (data not shown). Immunofluorescent confocal microscopy of double-labeled sections showed a high degree of overlap between sst_4-Li and SS-14-Li in many brain regions, including the cerebral cortex, striatum, and nucleus accumbens. High-power magnification revealed that sst_4-immunoreactive dendrites were often closely apposed by, but not cocontained within, SS-14-containing fibers and terminals (Fig. 6*A–F*,*J*). One notable exception was the hilar region of the dentate gyrus in which immunoreactive sst_4 receptors appeared to decorate processes of SS-14-positive interneurons. The fusiform cell bodies and very proximal portion of dendrites of these interneurons were intensely labeled for somatostatin immunoreactivity, whereas sst_4-Li was localized to the adjacent more distal portions of these dendrites and their ramifications within the hilus (Fig. 6*I*,*K*).

Spatial relationship of somatostatin receptor 4 to other somatostatin receptor subtypes

Finally, we examined the spatial relationships between sst_4 and the sst_{2A}, sst_{2B}, and sst_3 receptors, all of which are abundant in the same forebrain regions. As shown in Figure 7*A–C*, sst_{2A}-Li was

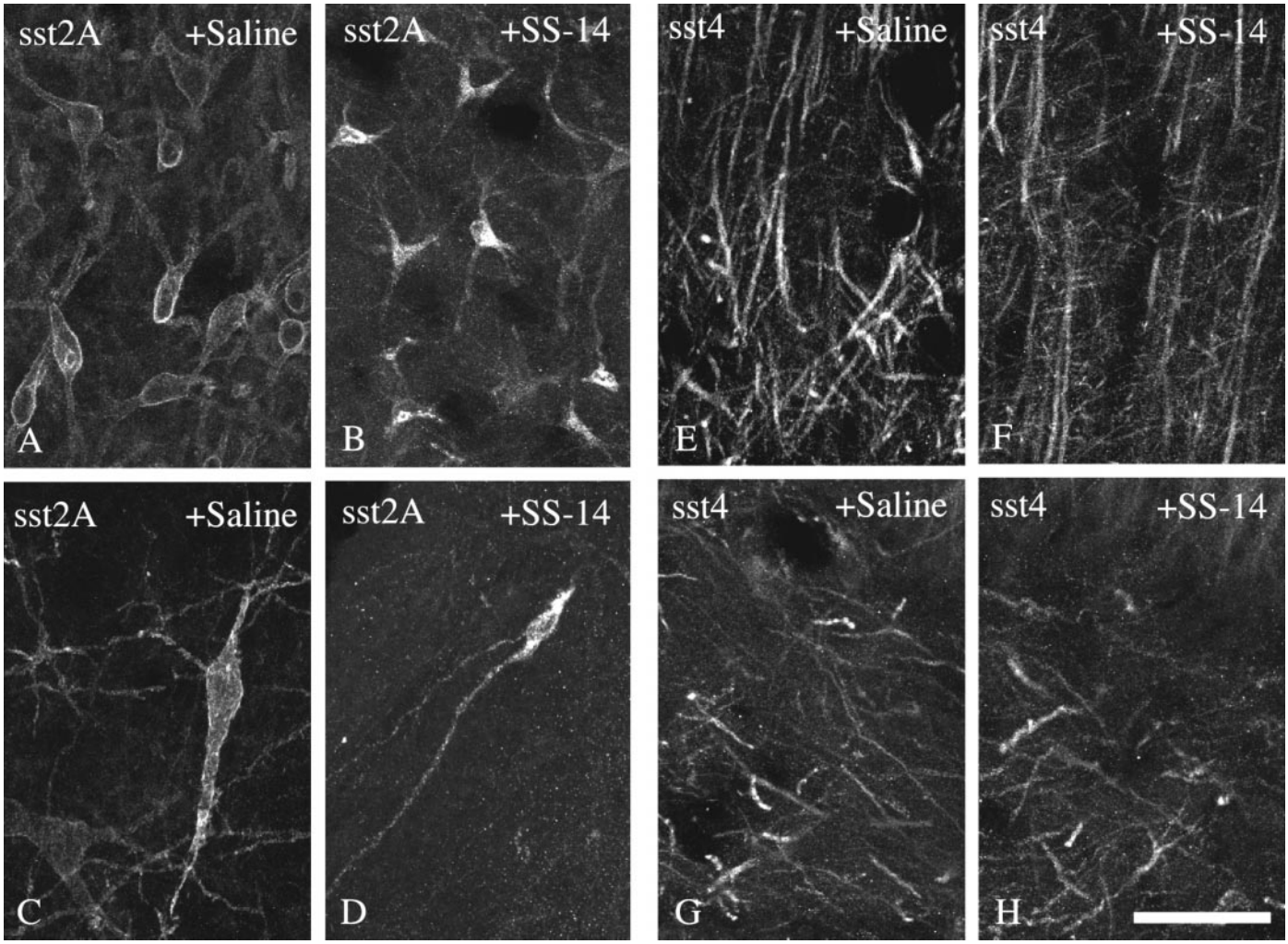

Figure 8. Differential internalization of sst_{2A} and sst_4 in rat brain. Confocal micrographs showing the subcellular distribution of sst_{2A}-Li (*A–D*) and sst_4-Li (*E–H*) in rat brain after intracerebroventricular administration of either saline (*A*, *C*, *E*, *G*) or 1 μg of SS-14 (*B*, *D*, *F*, *H*). Coronal rat brain section immunofluorescently stained with affinity-purified anti-sst_{2A} (6291) (*A–D*) or anti-sst_4 (6002) (*E–H*) antibodies. Micrographs shown in *A* and *B* were taken from the lateral septum, *C* and *D* were taken from the central gray, *E* and *F* were taken from the cortex, and *G* and *H* were taken from the hilar region of the dentate gyrus. Note that sst_{2A} rapidly redistributes from the plasma membrane into vesicle-like structures within the cytosol. In contrast, sst_4 appears to be resistant against short-term downregulation via receptor internalization. Scale bar: *A–H*, 25 μm.

prominent on fibers in the stratum oriens and radiatum of the hippocampal CA1. Although sst_4-Li appeared to be in a similar position, no colocalization was observed between these two receptors (Fig. 7*J*). In contrast, a high degree of colocalization was seen between sst_4-Li and sst_{2B}-Li in layer V cortical pyramidal cells (Fig. 7*D–F*). Interestingly, these two receptors differ in their subcellular targeting. Whereas sst_{2B}-Li was distributed in a patch-like manner at the plasma membranes of the soma and proximal dendrites, sst_4-Li was most dense at the distal portion of the apical dendrites of these neurons (Fig. 7*K*). The sst_3 receptor is also abundant in the cerebral cortex. Whereas sst_3-Li is selectively targeted to neuronal cilia, sst_4-Li is most prominent in the dendritic domain of a subpopulation of cortical neurons. Nevertheless, a colocalization of these two receptors was not evident (Fig. 7*G–I*).

The sst_4 receptor does not undergo agonist-promoted internalization *in vivo*

The sst_4 receptor is unique among somatostatin receptors in that it appears to be resistant against agonist-induced internalization when expressed in HEK 293 cells (Kreienkamp et al., 1998). Because heterologous expression of sst_4 results in a receptor protein that is either not or incompletely glycosylated (Fig. 2), it is important to determine agonist-induced endocytosis of the native receptor. When SS-14 was administered intracerebroventricularly and the subcellular distributions of the sst_4 and sst_{2A} receptors were monitored immunocytochemically, we found that the sst_{2A} receptor redistributed rapidly from the plasma membrane into vesicle-like structures in the cytosol (Fig. 8*A–D*). However, such a redistribution was not seen for the sst_4 receptor (Fig. 8*E–H*).

In primary neuronal cultures native sst_4 and sst_{2A} receptors were readily detectable by immunofluorescence using somatostatin receptor subtype-specific antibodies. When these cultures were exposed to SS-14, the membrane-bound sst_{2A} receptors were progressively lost. After 45 min, nearly all sst_{2A} receptors redistributed from the plasma membrane into the cytosol (Fig. 9, *top panel*). In contrast, such a loss of membrane-bound receptor with a concomitant accumulation of receptors in the cytosol was not

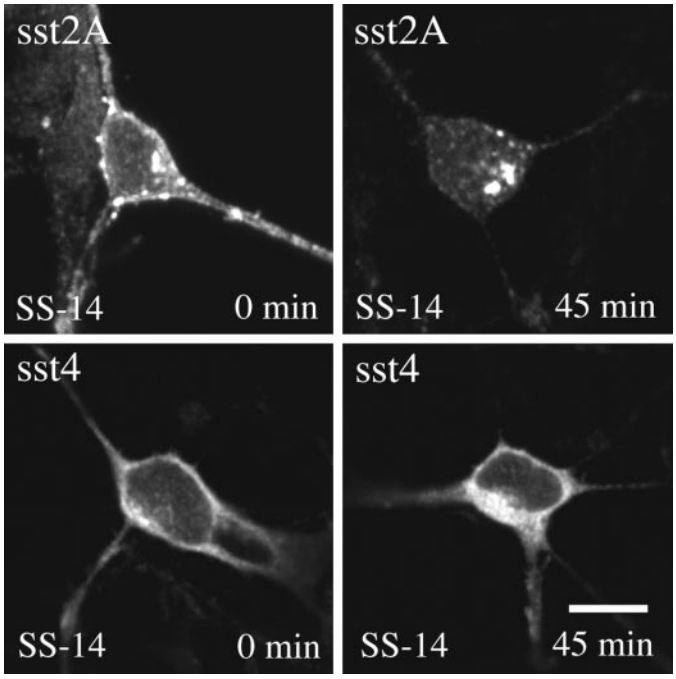

Figure 9. Differential internalization of sst_{2A} and sst_4 in primary neuronal culture. Primary dissociated cultures were prepared from embryonic day 19 fetuses and grown on coverslips for 1–2 weeks. Cells were then exposed to 100 nM SS-14 for 0 or 45 min. Cells were subsequently fixed, fluorescently labeled with antibodies specific for either sst_{2A} or sst_4, and examined by confocal microscopy. Note that nearly all immunoreactive sst_{2A} receptors rapidly redistribute from the plasma membrane into the cytosol in the presence of somatostatin. Such a redistribution was not seen for the sst_4 receptor. Very similar results were obtained in the presence of monensin. Representative results from three independent experiments performed in duplicate. Scale bar, *A–D*, 25 μm.

seen for the sst_4 receptor (Fig. 9, *bottom panel*). Very similar results were obtained in the presence of monensin, an inhibitor of endosomal acidification, which blocks receptor recycling (data not shown).

Dynamic changes of sst_4-Li after percussion trauma of the cortex

Finally, we monitored time-dependent changes in sst_4-Li in an animal model of neurotrauma. As shown in Figure 10, 8 and 24 hr after traumatic injury, the immunoreactive sst_4 receptors progressively declined on the ipsilateral, but not on the contralateral, side of damage. This decline of neuronal sst_4 receptors coincided was an induction of sst_4 receptors in non-neuronal cells, as evidenced by their lack of colocalization with MAP-2. These cells exhibited a glial-like morphology and were present at 24 hr after neurotrauma at the sites of damage. The staining of these glial-like cells also appears to represent sst_4-Li because it was completely neutralized by preincubation of the antibody with its immunizing peptide (data not shown).

DISCUSSION

In the present study, we have raised anti-peptide antisera against the C-terminal tail of the sst_4 receptor. Several lines of evidence suggest that these antibodies react specifically with their targeted receptor. First, in immunodot-blot assays, the anti-sst_4 antisera specifically detected their cognate peptide but not the peptides corresponding to the C-terminal region of other somatostatin receptor subtypes. Second, immunocytochemical staining of transfected HEK 293 cells revealed that the anti-sst_4 antisera selectively stained cells expressing the appropriate receptor but did not stain wild-type cells or cells transfected with other somatostatin receptors. In fact, the staining pattern of the anti-sst_4 antibody, which detects the C terminus of the sst_4 receptor, was virtually identical to that seen with anti-T7 tag antibody, which detects the N-terminal added epitope tag, suggesting that both antibodies recognized the same receptor. Third, on Western blots, the affinity-purified antibody detected a band that migrated at ~70 kDa before and ~50 kDa after enzymatic deglycosylation in rat brain. This staining was neutralized by preincubation of the antibody with its cognate peptide. In stably transfected HEK 293 cells, only a single band of ~50 kDa was detected by both the anti-sst_4 antibody (6002) and the anti-T7 tag antibody. These data suggest that the sst_4 receptor heterologously expressed in HEK 293 cells, as well as in other expression systems, may be either nonglycosylated or only partially glycosylated (Helboe et al., 1997). In contrast, the native receptor expressed in rat brain appears to be heavily glycosylated. Fourth, the antibody revealed a unique staining pattern in brain tissue sections with prominent immunofluorescent in many forebrain regions. This immunostaining was completely abolished after preincubation of the antibody with the peptide (10 μg/ml) used to immunize the rabbits. Moreover, the regional pattern of sst_4-Li was largely consistent with the distribution of sst_4 mRNA reported by earlier *in situ* hybridization studies (Wulfsen et al., 1993; Bito et al., 1994; Harrington et al., 1995; Perez and Hoyer, 1995). Finally, the C-terminal peptide is likely to have served as sst_4-specific immunogen because this peptide was found to have amino acid identities no greater than 34% to other peptide sequences when aligned to current entries in the National Center for Biotechnical Information databases using BLAST 2.0.

Previous autoradiographic binding studies could not unequivocally identify the cellular location of the various somatostatin receptor subtypes in mammalian brain. High densities of binding sites were found in the olfactory bulb, cerebral cortex, dentate gyrus, CA1–CA3 subfields of the hippocampus, lateral septum, striatum, piriform cortex, and amygdala, a regional pattern that corresponds well with the distribution of sst_4-Li. The development of sst_4 receptor-specific antibodies provides a level of cellular resolution that allowed us to define the subcellular localization of the sst_4 receptor protein. In the CNS of adult rats, sst_4-Li was found on neuronal somata and dendrites. Somatodendritic targeting of the sst_4 receptor was confirmed by its frequent colocalization with dendritic, but not axonal or glial, markers. Moreover, at the electron microscopic level, sst_4-Li was exclusively confined to dendrites, symmetrical, and, in some instances, asymmetrical synapses, suggesting that the sst_4 receptor may be poised to mediate both inhibitory and excitatory postsynaptic responses of somatostatin.

This conclusion is supported by our finding that sst_4-Li and SS-14-Li show complementary distributions in many brain regions. Double-labeled immunofluorescent confocal microscopy revealed that sst_4-immunoreactive dendrites were often closely apposed by, but not cocontained within, SS-14-containing fibers and terminals, suggesting that SS-14 may be indeed a physiological relevant ligand for the sst_4 receptor. A different receptor–ligand relationship, however, was revealed in the hilar region of the dentate gyrus in which sst_4-Li decorated processes of SS-14-immunoreactive interneurons. These neurons have been described previously as HIPP cells (hilar interneurons projecting to the perforant path), with their dendritic arborizations confined to

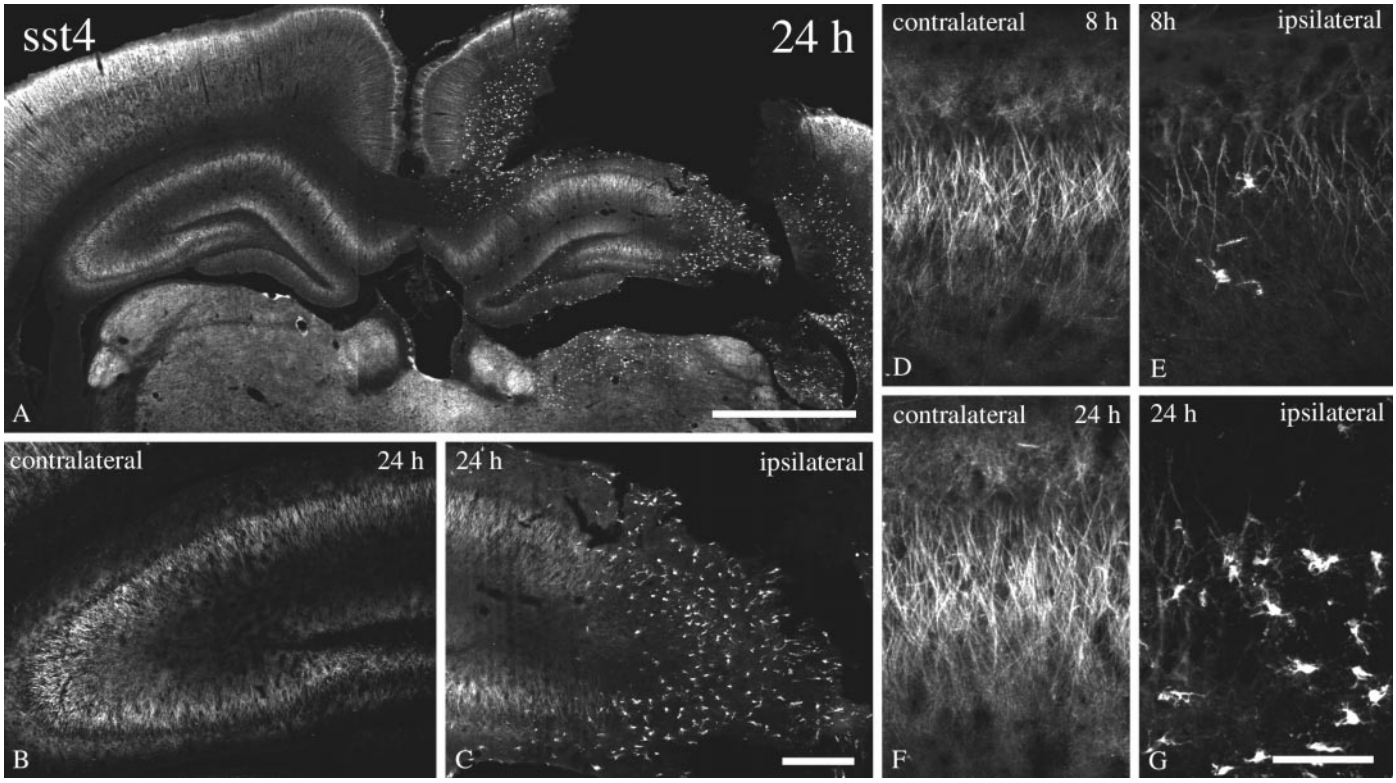

Figure 10. Dynamic changes of sst_4-Li after percussion trauma of the cortex. Immunofluorescent confocal micrographs of coronal rat brain section of animals that had been subjected to percussion of trauma of the cortex either 8 or 24 hr before vascular perfusion. All sections were stained with affinity-purified anti-sst_4 antibodies (6002). Note that, at 8 and 24 hr after traumatic injury, the immunoreactive sst_4 receptors progressively declined on the ipsilateral, but not on the contralateral, side of damage. This decline of neuronal sst_4 receptors coincided with an induction of sst_4 receptors in cells with a glial-like morphology. Scale bars: *A*, 250 μm; *B*, *C*, 50 μm; *D–G*, 10 μm.

the hilus and axons traveling to the outer third of the dentate gyrus molecular layer (Hökfelt et al., 1974; Johannson et al., 1984; Esclapez and Houser, 1995; Freund and Buzsaki, 1996). It is very tempting to speculate that sst_4 may function as an autoreceptor on these neurons. However, it is believed that SS-14 is mainly released from the axon terminals of these neurons and would thus have to diffuse over considerable long distances before it may activate the dendritic sst_4 receptor. To what extent SS-14 may be released from the dendrites of these interneurons is uncertain.

An interesting spatial relationship was also observed between sst_4 and sst_{2B}. Although both appear to be expressed by the same cortical pyramidal cells, sst_4 and sst_{2B} are being targeted to different postsynaptic sites. Whereas sst_{2B}-Li was distributed in a patch-like manner along the soma and proximal dendrites, sst_4-Li was most dense at the distal portion of the apical dendrites of these neurons (Schulz et al., 1998c; Schindler et al., 1999). Moreover, sst_4 and sst_3 mRNA have been reported to be coexpressed in cortical pyramidal cells (Perez and Hoyer, 1995). We have shown previously that the sst_3 receptor is selectively targeted to neuronal cilia (Händel et al., 1999). No more then one cilium originates from one neuronal cell body and extends into an intercellular pocket.

We have compared the agonist-induced internalization of the sst_4 receptor with the sst_{2A} receptor in two different *in vivo* models. Whereas the native sst_{2A} receptor was subject to rapid agonist-induced endocytosis, the native sst_4 receptor appeared to be resistant to short-term downregulation via receptor internalization. Previous mutagenesis experiments have demonstrated that the C-terminal tail of the sst_4 receptor may contain a negative regulatory motif for receptor internalization (Kreienkamp et al., 1998). In fact, the rat sst_4 receptor can be made sensitive to agonist-induced internalization by mutation of a single threonine (T331). Thus, the different ligand–receptor internalization profiles observed for two major postsynaptic somatostatin receptors may hold important clues for short- and long-term desensitization of somatostatin-mediated signals.

Somatostatin has been implicated in the modulation of complex behaviors, such as motor activity and memory formation (Matsuoka et al., 1994). In addition, levels of somatostatin are altered in several human brain dysfunctions, such as senile dementia of the Alzheimer type (Davies et al., 1980; Grouselle et al., 1998) and temporal lobe epilepsy (Robbins et al., 1991). Both inhibitory and excitatory effects have been reported for somatostatin on hippocampal and cortical neurons (Dodd and Kelly, 1978; Pittman and Siggins, 1981; Delfs and Dichter, 1983; Moore et al., 1988). Finally, electrophysiological studies have described postsynaptic and presynaptic actions of somatostatin (Boehm and Betz, 1997; Tallent and Siggins, 1997, 1999). Thus, the sst_4 receptor is well positioned to mediate postsynaptic somatostatin effects in these brain regions. However, delineation of the precise contribution of each of the somatostatin receptors to the modulation of complex behaviors would require subtype-selective agonists, which only recently have become available (Rohrer et al., 1998).

In addition, we show that sst_4 is strictly neuronal. However, we also show that, 24 hr after traumatic injury, the immunoreactive sst_4 receptors were also present on non-neuronal cells. These cells were selectively seen at primary and secondary sites of damage and, thus, may play a role in the neuronal degeneration–

regeneration process. Consequently, expression of sst_4 on these cells may offer the potential to modulate post-traumatic structural changes in the brain using sst_4-selective ligands.

In conclusion, the present study provides the first description of the distribution of immunoreactive sst_4 receptor proteins in mammalian brain. We show that sst_4 is strictly somatodendritic and most likely functions in a postsynaptic manner. Unlike sst_{2A}-mediated responses, the sst_4-mediated effects are not subject to short-term downregulation by receptor internalization. Finally, non-neuronal sst_4 receptors may have a previously unappreciated function during degeneration–regeneration processes.

REFERENCES

Bell GI, Reisine T (1993) Molecular biology of somatostatin receptors. Trends Neurosci 16:34–38.

Bernert H, Turski L (1996) Traumatic brain damage prevented by the non-*N*-methyl-D-aspartate antagonist 2,3-dihydroxy-6-nitro-7-sulfamoylbenzo[*f*]quinoxaline. Proc Natl Acad Sci USA 93:5235–5240.

Bito H, Mori M, Sakanaka C, Takano T, Honda Z, Gotoh Y, Nishida E, Shimizu T (1994) Functional coupling of SSTR4, a major hippocampal somatostatin receptor, to adenylate cyclase inhibition, arachidonate release, and activation of mitogen-activated protein kinase cascade. J Biol Chem 269:12722–12730.

Boehm S, Betz H (1997) Somatostatin inhibits excitatory transmission at rat hippocampal synapses via presynaptic receptors. J Neurosci 17:4066–4075.

Brazeau P, Vale W, Burgus R, Ling N, Butcher M, Rivier J, Guillemin R (1973) Hypothalamic polypeptide that inhibits the secretion of immunoreactive pituitary growth hormone. Science 179:77–79.

Bruno JF, Xu Y, Song J, Berelowitz M (1992) Molecular cloning and functional expression of a brain-specific somatostatin receptor. Proc Natl Acad Sci USA 89:11151–11155.

Davies P, Katzmann R, Terry RD (1980) Reduced somatostatin-like immunoreactivity in cerebral cortex from cases of Alzheimer disease and Alzheimer senile dementia. Nature 288:279–280.

Delfs JR, Dichter MA (1983) Effects of somatostatin on mammalian cortical neurons in culture: physiological actions and unusual dose response characteristics. J Neurosci 3:1176–1186.

de Lecea L, Criado JR, Prospero-Garcia O, Gautvik KM, Schweitzer P, Danielson PE, Dunlop CLM, Siggins GR, Henriksen SJ, Sutcliffe JG (1996) A cortical neuropeptide with neuronal depressant and sleep-modulating properties. Nature 381:242–245.

de Lecea L, Del Rio JA, Criado JR, Alcantara S, Morales M, Danielson PE, Henriksen SJ, Soriano E, Sutcliffe JG (1997) Cortistatin is expressed in distinct subset of cortical interneurons. J Neurosci 17:5868–5880.

Dodd J, Kelly JS (1978) Is somatostatin an excitatory transmitter in the hippocampus? Nature 273:674–675.

Dournaud P, Gu YZ, Schonbrunn A, Mazella J, Tannenbaum GS, Beaudet A (1996) Localization of the somatostatin receptor SST2A in rat brain using a specific anti-peptide antibody. J Neurosci 16:4468–4478.

Dournaud P, Boudin H, Schonbrunn A, Tannenbaum GS, Beaudet A (1998) Interrelationships between somatostatin sst2A receptors and somatostatin-containing axons in rat brain: evidence for regulation of cell surface receptors by endogenous somatostatin. J Neurosci 18:1056–1071.

Esclapez M, Houser CR (1995) Somatostatin neurons are a subpopulation of GABA neurons in the rat dentate gyrus: evidence from colocalization of pre-prosomatostatin and glutamate decarboxylase messenger RNA. Neuroscience 64:339–355.

Freund TF, Buzsaki G (1996) Interneurons of the hippocampus. Hippocampus 6:347–370.

Gillies G (1997) Somatostatin: the neuroendocrine story. Trends Pharmacol Sci 18:87–95.

Grouselle D, Winsky-Sommerer R, David JP, Delacourte A, Dournaud P, Epelbaum J (1998) Loss of somatostatin-like immunoreactivity in the frontal cortex of Alzheimer patients carrying the apolipoprotein epsilon 4 allele. Neurosci Lett 255:21–24.

Händel M, Schulz S, Stanarius A, Schreff M, Erdtmann-Vourliotis M, Schmidt H, Wolf G, Höllt V (1999) Selective targeting of somatostatin receptor sst3 to neuronal cilia. Neuroscience 89:909–926.

Harrington KA, Schindler M, Humphrey PP, Emson P (1995) Expression of messenger RNA for somatostatin receptor subtype 4 in adult rat brain. Neurosci Lett 188:17–20.

Helboe L, Moller M, Norregaard L, Schiodt M, Stidsen CE (1997) Development of selective antibodies against the human somatostatin receptor subtypes sst1–sst5. Brain Res Mol Brain Res 49:82–88.

Helboe L, Stidsen CE, Moller M (1998) Immunohistochemical and cytochemical localization of the somatostatin receptor subtype sst1 in the somatostatinergic parvocellular neuronal system of the rat hypothalamus. J Neurosci 18:4938–4945.

Helboe L, Hay-Schmidt A, Stidsen CE, Moller M (1999) Immunohistochemical localization of the somatostatin receptor subtype 2 (sst2) in the central nervous system of the golden hamster (*Mesocricetus auratus*). J Comp Neurol 405:247–261.

Hökfelt T, Efendic S, Johannson O, Luft R, Arimura A (1974) Immunohistochemical localization of somatostatin (growth-hormone release-inhibiting factor) in the guinea pig brain. Brain Res 80:165–169.

Holloway S, Feniuk W, Kidd EJ, Humphrey PPA (1996) A quantitative autoradiographical study on the distribution of somatostatin sst2 receptors in the rat central nervous system using (125 I)-BM-23027. Neuropharmacology 35:1109–1120.

Hoyer D, Bell GI, Berelowitz M, Epelbaum J, Feniuk W, Humphrey PPA, O'Carroll AM, Patel YC, Schonbrunn A, Taylor JE, Reisine T (1995) Classification and nomenclature of somatostatin receptors. Trends Pharmacol Sci 13:61–69.

Johannson O, Hökfelt T, Elde PR (1984) Immunohistochemical distribution of somatostatin-like immunoreactivity in the central nervous system of the adult rat. Neuroscience 13:265–339.

Kluxen FW, Bruns C, Lübbert H (1992) Expression cloning of a rat brain somatostatin receptor cDNA. Proc Natl Acad Sci USA 89:4618–4622.

Koch T, Schulz S, Schröder H, Wolf R, Raulf E, Höllt V (1998) Carboxyl-terminal splicing of the rat μ opioid receptor modulates agonist-mediated internalization and resensitization. J Biol Chem 273:13652–13657.

Kreienkamp HJ, Roth A, Richter D (1998) Rat somatostatin receptor subtype 4 can be made sensitive to agonist-induced internalization by mutation of a single threonine (residue 331). DNA Cell Biol 17:869–878.

Martin JL, Chesselet MF, Raynor K, Gonzales C, Reisine (1991) Differential distribution of somatostatin receptor subtypes in rat brain revealed by newly developed somatostatin analogs. Neuroscience 41:581–593.

Matsuoka N, Maeda N, Yamaguchi I, Satoh M (1994) Possible involvement of brain somatostatin in the memory formation of rats and the cognitive enhancing action of FR121196 in passive avoidance task. Brain Res 642:11–19.

Meyerhof W, Wulfsen, I, Schönrock C, Fehr C, Richter D (1992) Molecular cloning of a somatostatin-28 receptor and comparison of its expression pattern with that of somatostatin-14 receptor in rat brain. Proc Natl Acad Sci USA 89:10267–10271.

Moore SD, Madamba S, Joels M, Siggins GR (1988) Somatostatin augments the M-current in hippocampal neurons. Science 239:278–280.

O'Carroll AM, Lolait SJ, Konig M, Mahan LC (1992) Molecular cloning and expression of a pituitary somatostatin receptor with preferential affinity for somatostatin-28. Mol Pharmacol 42:939–946.

Papa M, Bundman MC, Greenberger V, Segal M (1995) Morphological analysis of dendritic spine development in primary cultures of hippocampal neurons. J Neurosci 15:1–11.

Perez J, Hoyer D (1995) Co-expression of somatostatin SSTR-3 and SSTR-4 receptor messenger RNAs in the rat brain. Neuroscience 64:241–253.

Pittman QJ, Siggins GR (1981) Somatostatin hyperpolarizes hippocampal pyramidal cells *in vitro*. Brain Res 221:402–408.

Robbins RJ, Brines ML, Kim JH, Adrian T, deLannerolle N, Welsh MS, Spencer DD (1991) A selective loss of somatostatin in the hippocampus of patients with temporal lobe epilepsy. Ann Neurol 29:325–332.

Rohrer L, Raulf F, Bruns C, Buettner R, Hofstaedter F, Schule R (1993) Cloning and characterization of a fourth human somatostatin receptor. Proc Natl Acad Sci USA 90:4196–4200.

Rohrer SP, Birzin ET, Mosley RT, Berk SC, Hutchins SM, Shen DM, Xiong Y, Hayes EC, Parmar RM, Foor F, Mitra SW, Degrado SJ, Shu M, Klopp JM, Cai SJ, Blake A, Chan WW, Pasternak A, Yang L, Patchett AA, Smith RG, Chapman KT, Schaeffer JM (1998) Rapid identification of subtype-selective agonists of the somatostatin receptor through combinatorial chemistry. Science 282:737–740.

Roth A, Kreienkamp HJ, Meyerhof W, Richter D (1997) Phosphorylation of four amino acid residues in the carboxyl terminus of the rat somatostatin receptor subtype 3 is crucial for its desensitization and internalization. J Biol Chem 272:23769–23774.

Schindler M, Sellers LA, Humphrey PPA, Emson PC (1997) Immunohistochemical localization of the somatostatin sst2(A) receptor in the rat brain and spinal cord. Neuroscience 76:225–240.

Schindler M, Humphrey PP, Lohrke S, Friauf E (1999) Immunohistochemical localization of the somatostatin sst2(b) receptor splice variant in the rat central nervous system. Neuroscience 90:859–874.

Schulz S, Schulz S, Schmitt J, Wiborny D, Schmitt H, Olbricht S, Weise W, Roessner A, Gramsch C, Höllt V (1998a) Immunocytochemical detection of somatostatin receptors sst1, sst2A, sst2B and sst3 in paraffin-embedded breast cancer tissue using subtype-specific antibodies. Clin. Cancer Res 4:2047–2052.

Schulz S, Schreff M, Schmidt H, Händel M, Przewlocki R, Höllt V (1998b) Immunocytochemical localization of somatostatin receptor sst2A in the rat spinal cord and dorsal root ganglia. Eur J Neurosci 10:3700–3708.

Schulz S, Schmidt H, Händel M, Schreff M, Höllt V (1998c) Differential distribution of alternatively spliced somatostatin receptor 2 isoforms (sst2A and sst2B) in rat spinal cord. Neurosci Lett 257:37–40.

Sellers LA (1999) Prolonged activation of extracellular signal-regulated kinase by a protein kinase C-dependent and N17Ras-insensitive mechanism mediates the proliferative response of $G_{i/o}$-coupled Somatostatin sst_4 receptors. J Biol Chem 274:24280–24288.

Tallent MK, Siggins GR (1997) Somatostatin depresses excitatory but not inhibitory neurotransmission in rat CA1 hippocampus. J Neurophysiol 78:3008–3018.

Tallent MK, Siggins GR (1999) Somatostatin acts in CA1 and CA3 to reduce hippocampal epileptiform activity. J Neurophysiol 81:1626–1635.

Uhl GR, Tran V, Snyder SH, Martin JB (1985) Somatostatin receptors: distribution in rat central nervous system and human frontal cortex. J Comp Neurol 240:288–304.

Vanetti M, Kouba M, Wang X, Vogt G, Höllt V (1992) Cloning and expression of a novel mouse somatostatin receptor (SSTR2B). FEBS Lett 311:290–294.

Vanetti M, Vogt G, Höllt V (1993) The two isoforms of the mouse somatostatin receptor (mSSTR2A and mSSTR2B) differ in coupling efficiency to adenylate cyclase and in agonist-induced receptor desensitization. FEBS Lett 331:260–266.

Wulfsen I, Meyerhof W, Fehr S, Richter D (1993) Expression patterns of rat somatostatin receptor genes in pre-and postnatal brain and pituitary. J Neurochem 61:1549–1552.

Yamada Y, Post SR, Wang K, Tager HS, Bell GI, Seino S (1992) Cloning and functional characterization of a family of human and mouse somatostatin receptors expressed in brain, gastrointestinal tract, and kidney. Proc Natl Acad Sci USA 89:251–255.

Yasuda K, Rens-Domiano S, Breder CD, Law SF, Saper CB, Reisine T, Bell GI (1992) Cloning of a novel somatostatin receptor, SSTR3, coupled to adenylylcyclase J Biol Chem 267:20422–20428.